



Electro-Mechanical Characterization of Graphite/Epoxy Composites as Potential External-Layer Material for Antenna Radome

Ekale Aruma^{1,2}, Waweru Njeri², Joseph Muguro²

¹ Moi University, 3900-30100 Eldoret, Kenya

² Dedan Kimathi University of Technology, 657-10100 Nyeri, Kenya

ARTICLE INFORMATION

Received: June 12, 2025

Revised: September 17, 2025

Accepted: November 3, 2025

Available online: Desember 1, 2025

KEYWORDS

Radome, Antenna, Composites, Surface resistivity, Tensile

CORRESPONDENCE

Phone: +254 705632796

E-mail: john.aruma19@students.dkut.ac.ke

A B S T R A C T

Graphite is widely recognized in electrical applications for its inherent conductivity. As a reinforcement in composite materials, graphite fibers greatly improve both strength and rigidity, making them ideal for constructing radomes. Traditionally, radomes used in ground and naval settings are made from high-cost materials, such as fiberglass, quartz, and aramid fibers, which are often combined with resins like polyester and epoxy. Nonetheless, issues in structural formation continue to pose challenges. This study aims to investigate the electrical and mechanical properties of graphite/epoxy composites using a dynamic mechanical analyzer (DMA) in double cantilever mode, in accordance with ASTM D7028-07 standards. The objective is to prepare epoxy/graphite composites on a high-density polyethylene (HDPE) substrate with varying composition levels. The study further aims to evaluate the electrical and mechanical properties of electrostatic discharge (ESD) composites using the dynamic materials testing (DMT) method, with a focus on analyzing graphite-epoxy composites as an external layer on antenna radomes. Various specimen types—pure epoxy, surface-coated, and mixed samples with different graphite particle concentrations—were tested at temperatures from 0 to 140°C. A 30V voltage was applied to each specimen, and the resulting current and sheet resistivity were recorded. The electro-mechanical and viscoelastic properties were analyzed, revealing that stress-induced plastic flow occurred in some specimens, accompanied by increased strain energy in graphite-weighted samples. Surface-coated specimens demonstrated distinct behavior, while mixed samples showed a linear strain energy increase up until fracture. Conductivity in epoxy composites was affected by filler content, with conductivity improvements up to a certain filler percentage.

INTRODUCTION

A radar antenna emits a radar wave into air which must travel through a material between a radar sensor and the desired target, the material between is radome. A radome (radar + dome) an enclosure for a radar antenna, designed to be electromagnetically transparent, structurally strong, and resistant to environmental conditions. In radome design, knowledge of signal-to-noise ratio (SNR) budget must be established and electrical properties of transmissivity, reflection and diffraction must be factored.

Electromagnetic wave reflections occur at the boundaries of the plane mismatch, the plane in this case considered as boundary of two media with different dielectric properties and different permittivity. The interaction leads to reflection and transmission of waves at the boundary of medium, quantized of reflection coefficient and transmission coefficient. Reflection coefficient is the ratio of reflected incident electric field strength, and transmission coefficient being the ratio of transmitted and incident electric field strength shown in the Equations ...

$$\Gamma = \frac{E_r}{E_i} = \frac{\sqrt{\epsilon_1} - \sqrt{\epsilon_2}}{\sqrt{\epsilon_1} + \sqrt{\epsilon_2}} \quad (1)$$

$$\tau = \frac{E_t}{E_i} = \frac{2\sqrt{\epsilon_1}}{\sqrt{\epsilon_1} + \sqrt{\epsilon_2}} \quad (2)$$

Radomes can be constructed in several shapes such as planar, spherical and geodesic where the shape influences the radiation pattern or field of view (FOV) and maximum achievable distance by radar sensor inside a radome. Material choice such as fiberglass, PTFE-coated fabric, and polycarbonate generally is dependent on the targeted application environmental use. In design, for instance, metals render high attenuation for Electromagnetic wave propagation, attributed to skin effect. To estimate losses similar to the absorption in a dielectric loss, skin effect shows an exponential decay over the length in the material. Avoidance of poor dielectrics with high loss tangents and high permittivity is preferable. Consequently, design of a radome ideally with less than 2 to 3dB is desirable. Spacing between the radar antennas and the radome is paramount, radomes in the near-field always impact performance. The following theoretical Equations demonstrate aspect of distance on magnetic, electromagnetic power and skin depth principle utilized in design

of Radome. Magnetic field strength depends on the distance in the conductor: -

$$H(x) = H(x = 0)e^{-\frac{x}{\delta}} \quad (3)$$

Electromagnetic power depending on the distance in the conductor: -

$$P(x) = P(x = 0)e^{-\frac{2x}{\delta}} \quad (4)$$

With the skin depth: -

$$\delta = \sqrt{\frac{2\rho}{\omega\mu}} = \sqrt{\frac{2}{2\pi f \sigma \mu_0 \mu_r}} \quad (5)$$

In a far-field case radar has to penetrate through obstacles which would results to losses, while near-field scenario is applicable when distance to antenna

$$< \frac{2D}{\lambda}, \quad (6)$$

For instance, in a single patch antenna with a ground plane of λ by λ underneath it, the border between near-field and far-field is at 2λ . Material placed in the near-field of a radar sensor, will influence the antenna, consequently antenna impedance will impact the transmitted and received power. Radome wall thickness helps in achieving optimum performance of the sensor or antenna, it's imperative that the wall thickness is equal to integer multiple $\lambda/2$ to enable radome to be near perfectly transparent for an intended range. Radome thickness is given in Equation 7, the wavelength in the material becomes shorter vs free air being an inverse function of the materials' dielectric constant in Equation 8.

$$t_{optimal} = \frac{n \cdot \lambda_m}{2} \quad (7)$$

$$\lambda_m = \frac{c}{f \cdot \sqrt{\epsilon_r}} \quad (8)$$

Radome is used in ground-based systems as well as modern avionics in military aircraft and missiles [1], [2], [3], antenna radomes play a crucial role in protecting sensitive electronic components of communication systems from harsh environmental conditions, such as extreme temperatures, moisture, and electromagnetic interference [4], [5], [6]. The choice of materials for radome construction significantly influences the overall performance and longevity, impacting signal transmission and reception efficiency. Recently, there has been a growing interest in using advanced composite materials to enhance radome structural and electromagnetic properties [2], [7], [8].

Graphite/epoxy composites have emerged as promising candidates for radome applications due to their unique mechanical strength, low weight, and excellent electrical properties[9], [10].

The inherent characteristics of graphite, with its high electrical conductivity and thermal stability, when combined with the structural advantages offered by epoxy resins, make these composites particularly appealing for antenna radome design. However, to ensure their successful integration into radome structures, a comprehensive understanding of the electro-mechanical behavior of graphite/epoxy composites is imperative [11], [12]

Silica's significance as a raw material was underscored, urging the exploration of alternative production processes from renewable sources [13], The study emphasized cyclic lifetime

assessment and effective recycling strategies, aiming for sustainable and cyclic production processes. Comparative analysis of silica extraction methods, types, and stability of resulting nano silica materials provided insights into potential large-scale production and hybrid/composite materials from alternative sources [13].

Carbon fibre-reinforced plastic (CFRP) composites properties were investigated using dynamic mechanical thermal analyzer in a single cantilever mode to expound on its properties on discontinuous asymmetric helicoidal carbon as a function of fiber architecture, study highlighted the adverse effects of hygrothermal ageing and minor pitch angles on viscoelastic properties, impacting energy absorption and dissipation capacities [14], [15].

There is an urgent need to develop new-generation radome materials, with a focus on understanding and enhancing their dielectric and mechanical properties, particularly for applications in hypersonic radome materials and metamaterial design[16] [17], [18], [19]. Introducing polymethyl methacrylate (PMMA) particles as a pore-forming agent has shown that controlled porosity in silicon nitride ceramics can reduce flexural strength at specific weight percentages while improving dielectric properties[20]. In radome design, balancing enhanced electromagnetic properties with mechanical durability is essential. Studies on multilayer structures and graded porosity effects suggest that silicon nitride ceramics with controlled porosity have potential as high-temperature radome materials for supersonic applications [17], [18],[21].

In electrochemical applications, increasing the graphite content in epoxy-graphite composites enhances both tensile strength and Young's modulus, providing valuable insights into their conductivity and mechanical behaviour [22]. Different materials cater to specific needs; for instance, high-temperature ceramic radomes (HTCR) are ideal for military vehicles due to their high-temperature resistance, low dielectric constant, low loss tangent, and robust structural integrity [23], [24], [25].

Each material offers distinct advantages: high-purity alumina boasts exceptional mechanical durability but lacks radar transparency, whereas fused silica exhibits excellent dielectric and mechanical properties but is vulnerable to erosion from rainfall [19].

Consequently, a robust radome design incorporates porosity concepts and a functionally graded porous structure into modern radome materials to optimize and enhance dielectric properties. Key factors in radome manufacturing include temperature resistance, tensile strength, dielectric constant, loss tangent, and porosity [1], [6]. Carbon fibre-reinforced polymer (CFRP) meshed shell radomes, with an overall stressed-skin structure, has to undergo tests involving stress, strain performance, and wind pressure on the radome.

The study [28], performed using composite radomes, revealed a safety margin for carbon fibre bending strength limit (T300) compared to those without. However, this did not address the effect on sheet resistivity[27], [28].

A review of composite materials for supersonic aircraft radomes in [19] [9], highlighted that polymer matrix composites offered excellent fatigue and corrosion resistance while being stiff and strong for different applications. The advantages of composites in this application lay in their low dielectric constant and low loss in radar transparency while maintaining high strength. Optimal material choices for radome fabrication necessitated the highest degree of property optimization for the efficient functionality of radar systems in supersonic aircraft [17]. Using sandwich structures in polymeric composites resulted in a 30% reduction in aircraft weight, thereby improving range and payload. Carbon fibre-reinforced polymer composites, analyzed through dynamic mechanical analysis (DMA), showed that viscoelastic properties were adversely affected by hygrothermally aged minor pitch angles but not major ones [14], [31]

Ceramic radome materials hold potential for applications in meta-materials design. In high-temperature environments, an ideal radome material has to possess flexural strength, a low dielectric constant, a low loss tangent, and high resistance to corrosion and thermal shock. Currently, no single material is considered ideal for hyper-sonic radomes. Dielectric properties are influenced by factors such as temperature, grain size, per cent porosity, and frequency. At the same time, ceramic materials were favored for radome applications due to their high operating temperatures, good dielectric properties, and strong mechanical characteristics [11], [12]

The effect of fillers on the electrical conductivity of epoxy composite materials was investigated by comparing predictive models, including Maxwell and Wider Mann Franz laws. The study, derived from the kinetic theory of gases in solid-state physics, established that the electrical conductivity of epoxy composites increased proportionately with an increase in filler quantity [17], [32].

In microwave materials, critical properties and applications in antennas, filters, and oscillators in the military and aerospace sectors involved radomes containing dielectric materials. These materials exhibit characteristics such as ease of passage of minimum transmission loss, dependence on dielectric constants, and loss of tangent. Ease of fabrication required considering material mechanical properties, including density, strength, and durability [24], [33]. These materials have to withstand environmental and contamination conditions without degradation. The properties have enabled the extensive use of microwave dielectric materials in terrestrial and satellite communications. Emerging microwave materials in the form of inks, composites, and foams were expected to provide future solutions [19].

Advancements in the Internet of Things (IoT), microwave technology, telecommunications, satellite broadcasting, and intelligent transport systems (ITSs) have led to increased demand for low-loss dielectric materials and electromagnetic interference (EMI) shielding materials. This heightened demand has expanded the knowledge of radome applications in microwave materials [7], [16], [34].

In a study on the bulk microstructure of epoxy-graphite composites using impulse acoustic microscopy, established that

epoxy composites filled with 1wt.% - 2wt.% exfoliated graphite (1-2 wt.% EG), were suitable materials for producing electromagnetic coatings for microwave and terahertz frequencies, with acceptable mechanical and thermal properties [35], [36], [37]. Adding fly ash at different weight percentages enhanced the mechanical properties of epoxy/graphite composites compared to pure epoxy. This enhancement was attributed to increased uniform dispersion, better adhesion, and strong inter-facial applications, where the cost of the system needed to be more economical [38]. A study on the dielectric properties of graphite-based epoxy composites in [28], filled with different kinds of graphite particles, including exfoliated, natural, coarse, medium, and fine artificial graphite in various temperature and frequency ranges, revealed that dielectric permittivity strongly increased with graphite particle size [40], [41].

At higher temperatures, electrical conductivity due to the finite electrical conductivity of the polymer matrix and electron tunnelling from the polymer matrix to graphite particles occurs in all composites. Exfoliated graphite (EG) was identified as the only effective additive among the various graphite particles. In terms of electromagnetic interference shielding composite materials, it was found that 2wt% of EG in epoxy was not transparent to electromagnetic radiation at 30 GHz [42].

An investigation into the structural characteristics, mechanical and dielectric properties of nanocomposites showed that dielectric constants of composites increased with the addition of graphite nanosheet content lower than 3.5 wt.% graphite filler content in [43]. The composites' tensile strength and storage modulus increased with increasing nanosheet concentration. Incorporating graphite nanosheets improved both the toughness and storage modulus of the composites. Inter facial action between graphite fillers and the epoxy matrix resulted in a higher tensile strength of epoxy/graphite nanosheet composites than that of pure epoxy resin. Increasing the content of graphite nanosheets resulted in a storage modulus that was 35% higher than the pure epoxy when the filler content reached 3wt.%. The interfacial interaction improved both dielectric and mechanical properties [20].

Advance search of potential nanocomposites and nanoparticles in search of application in materials science has led to diatoms research. This would lead to various applications in Radomes which would exist in different types depending on the conditions of use. Superior use seeks high strength, thermal stability, lightweight, low thermal expansion, chemical stability, low dielectric constant, and high stiffness [24]. Increased filler content showed improved tensile and Young's modulus and increased electrical conductivity at different frequencies. Electrical and mechanical properties of expanded/high-density polyethylene nanocomposites showed variance in electrical conductivity values observed using diffraction patterns. [3], [45], [46], [47].

Radomes are affected by temperature and other environmental conditions. In the market, radome materials were mostly researched for application in extreme conditions, i.e., extremely high and low temperatures, which altered the material characteristics of radomes.

Various radome materials have been studied, including Pyro Ceram 9606, Ray Ceram, slip-cast fused silica, dense and low-density silicon nitride, celsian, Nitroxyceram, Atrium silicate ceramics, and phosphate ceramic composites. However, epoxy/graphite remains relatively unexplored, particularly regarding its mechanical strength, electrical properties (dielectric and resistivity characteristics), loss tangent ($\tan \delta$), and temperature effects, especially in relation to commonly used radome types [48], [49].

Research on radome materials spans a wide range of options and factors, including advanced composites such as graphite/epoxy and silicon nitride ceramics, as well as the structural and electromagnetic behaviour of radome under varying conditions. These studies provide essential insights for optimizing radome materials to improve performance and durability across diverse applications. [15], [50], [51].

This study aims to investigate the electro-mechanical properties of graphite/epoxy composites using a dynamic material analyzer (DMA) operating in double cantilever mode. Adhering to ASTM standards, to comprehensively characterize the behavior of these composites under various conditions, with a particular focus on temperatures ranging from 0 to 140°C. Applying a 30V voltage to various specimen (mixed and surface coated) allows for the examination of sheet resistivity, offering insights into the electrical conductivity of the composite, These electrical parameters were essential for a comprehensive analysis of the electrical conductivity of the epoxy/graphite composites.

Our objective is to assess the potential of graphite/epoxy composites as external layer materials for antenna radomes, considering their nonlinearity, strain energy, and fracture characteristics. The findings of this study contribute to ongoing efforts to enhance the performance and durability of antenna systems through innovative material selection and engineering on radome design.

METHOD

This section discusses electro-mechanical characterization of graphite-epoxy composites as potential external layer for antenna radome procedures.

The preparation of epoxy/graphite powder composites on a High-Density Polyethylene (HDPE) substrate involved varying portions of the constituents.

A carefully curated selection of precise and specialized instruments was meticulously chosen for this study to enable comprehensive and accurate testing of the epoxy/graphite composites, as detailed in Table 1. This deliberate selection process considered the specific requirements of the materials and the range of properties to be measured, ensuring that each instrument used is suitable for capturing nuanced mechanical and electrical responses. The careful choice of these instruments and materials guarantees that the experimental setup is fully equipped to deliver highly dependable, precise, and detailed mechanical and electrical characterizations of the materials under investigation. This rigorous setup plays a crucial role in maintaining the consistency and validity of the results obtained,

thereby strengthening the overall reliability and reproducibility of the study.

Table 1 Instrument Table

NO		TYPE	PURPOSE
1.	Dynamic mechanical Testing analysis Machine (DMTA) DMA80 TA	Instrument	Specimen testing of modulus, damping factor, and polymer's structure-property relationship.
2.	Instron Dynamic Tensile Test Machine 8802	Instrument	fatigue testing of composite coupons and structures
3.	Keysight-Triple Output Programmable power supply EDU36311A DC 6-30V	Instrument	Setting Input Voltage
4.	Keysight -5 ½ Digital Multimeter EDU34450A	Instrument	Current across the specimen
5.	High density polyethylene polymer (HDPE)	Material	
6.	Graphite (carbon powder)	Material	
7.	Epoxy Araldite	Material	
8.	Digital Calipers	Instrument	Sylac Inductive System
9.	Rexel Class cut CL200	Instrument	Mixture cutter
10.	Surface Resistance meter ANT093-0050	Instrument	Resistivity measurement across the specimen.
11.	Specimens 10-samples of each, Categories of Mixtures and Surface coated (Wt.% Graphite vs Epoxy; 0,1,2,3, 3, 5, 7, 9) total of 70 Specimen samples		

Experimental Procedure

The experimental procedure employed in this study involved a systematic series of steps designed for the preparation of High-Density Polyethylene (HDPE) substrate. Figure 1 (a) and (b) show the High-Density Polyethylene (HDPE) substrate and Epoxy wt. 100% respectively.

1. HDPE substrate cleaned in preparation for the mixture.
2. Epoxy resin mixed within a time frame of 3mins.
3. Graphite measured into different wt.% content.
4. The graphite powder spread on the HDPE substrate.

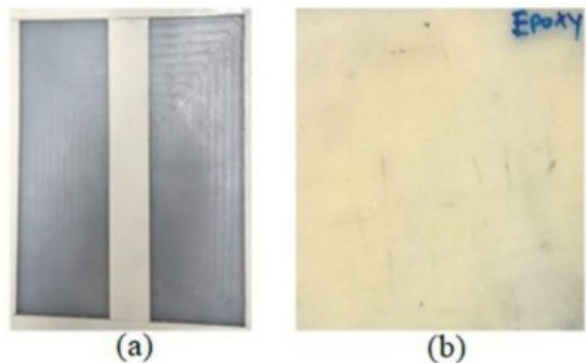


Figure 1 a) High-density polyethylene (HDPE) substrate b) Epoxy

Dynamic Mechanical Analysis (DMA) Tests

Dynamic Mechanical Analysis (DMA) is a crucial analytical technique employed to investigate the dynamic mechanical properties of materials as a function of temperature, time, frequency, and applied stress. This method offers valuable insights into a material's viscoelastic behavior, revealing how it responds to mechanical forces under changing conditions. DMA is particularly useful in characterizing the thermochemical properties of composites, such as the storage modulus and loss modulus, providing a comprehensive understanding of the material's mechanical performance across various temperatures. In this study, DMA was employed using the DMA Q 800 Analyzer from TA Instruments, USA, to explore and quantify the dynamic mechanical response of Epoxy/graphite composites, shedding light on their suitability for specific and sought applications as shown in Figure 2.

To conduct DMA analysis, the following steps were utilized:

1. Measure test specimen samples/Sheets
2. (n = 3) dimensions 12cm * 6cm * 0.5cm (Length X Width X Thickness), to determine thermochemical properties.
3. Place samples into the DMA Machine, test in a temperature range of 0-140 °C at a heating rate of 2 °C/Min.
4. Perform DMA tests of Epoxy/graphite composites on DMA Q 800 Analyzer (TA Instruments, USA).
5. Record results.



Figure 2 DMA Test set-up

Tensile Measurements

Tensile measurements assess the mechanical strength and performance of materials under applied forces. This information is vital for evaluating the structural integrity and durability of Epoxy/graphite composites. Tensile strength, modulus, and other mechanical properties are key factors in determining how well the material can withstand external forces, ensuring its suitability for application. Specimen and setup in Figures 6a and b, respectively. The following steps were used to measure tensile:-

1. Use Rexel Class cut CL200 Mixture cutter, cut specimens stripes by 12cm X 2cm at least 3 specimens (n=3) per wt.%, as seen in Figure 6(a).
2. Using digital calipers take and record measurements appropriately.
3. Repeat steps I and ii for Pure epoxy, Mixture (Epoxy/Graphite), and surface coated (Epoxy/Graphite) specimen.

4. Tape edges of the specimen at length of 2cm from both ends for holding by DMTA- DMA80 as shown in Figure 6 (b).
5. Carefully insert and grasp the specimen between the holders of DMTA- DMA80.
6. Capture the effect using DMTA Wave Matrix 2 data acquisition software and save plots.

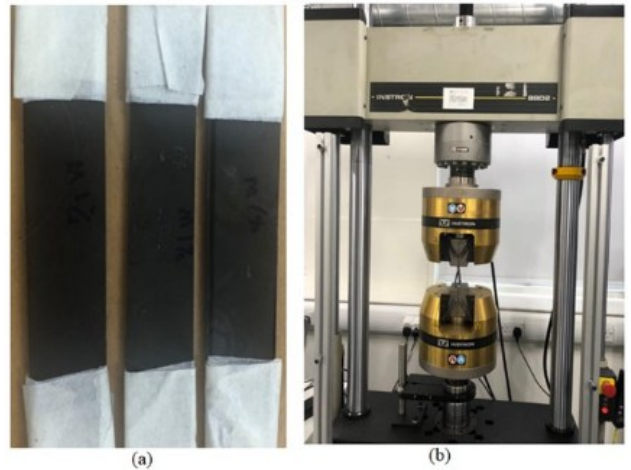


Figure 6 (a) Specimen (b) Instron Dynamic Tensile Test Machine 8802

Current Measurement During Tensile Tests

Current measurements during tensile tests are important in gaining insights into the electrical behavior of epoxy/graphite composites under stress. By connecting the specimens to an Instron tensile machine and utilizing a programmable power supply and digital multimeter, the test effectively captures the current trends until the specimen fractures.

The process helps to assess the material's electrical conductivity under varying tensile forces. Understanding the relationship between mechanical stress and electrical properties is crucial for applications where these composites are utilized, such as in radome designs. The data obtained from current measurements enhances the overall comprehension of the material's performance, enabling more informed decisions in engineering and design processes. The following process is followed in the current measurement during Tensile tests:

1. Connect each specimen to the Instron DMTA- DMA80 tensile machine.
2. Connect Keysight-Triple Output Programmable power supply EDU36311A DC 6-30V and set the voltage rating to max i.e. 30V
3. Using Keysight -5 ½ Digital Multimeter EDU34450A, measure current and capture current samples of 200 or until the specimen fractures.
4. Plot and save the current trends for each specimen.

Surface Sheet Resistivity Measurement

Sheet resistivity is a critical parameter for materials used in electronic applications, such as Epoxy/graphite composites. Sheet resistivity impacts radome design by reducing reflection of electromagnetic waves, higher resistance means the radome is more transparent to the radio waves. Helps in impedance

matching to that of the antenna further minimizing reflection thereby reduces the amount of electromagnetic energy absorbed. A radome with a high sheet resistivity can reduce reflection of electromagnetic waves. Higher resistance means its more transparent to the radio waves, allowing them to pass through with minimal disturbance.

In designing and utilizing thin-film coatings on radomes, Sheet resistivity is a key parameter when specific resistivities are required to enhance radar transparency or absorption. In material selection, considering sheet resistivity, dielectric constant, and mechanical strength is crucial; materials with low sheet resistivity are preferable, especially when transparency is a key consideration. Consequently, determines the ability of a material to conduct or resist the flow of electrical current.

Measuring sheet resistivity is crucial for understanding the electrical conductivity of the composite, which is essential in applications in external radome layers where electrical properties are significant. Figures 3-6 are specimens for testing. To conduct Surface sheet resistivity measurements, the following steps were followed:

1. Prepare surface-coated specimens with different weight percentages (wt.%) of epoxy/graphite substrates. The different weight percentages are wt.1%, wt.2%, wt.7%, wt.8% and wt.9% as shown from Figure 3 to Figure 6.
2. Dry the Specimen at normal room temperature.
3. Take and record ESD measurement from each specimen using surface resistance meter, then calculate the average.
4. Prepare mixed specimen(epoxy/graphite sheets) in different wt%.
5. Repeat steps ii and iii.



Figure 3 Epoxy/Graphite wt2% Surface coated

RESULTS AND DISCUSSION

Mechanical properties of Epoxy/Graphite composites

Several key parameters characterize the mechanical properties of Epoxy/Graphite composites. The storage modulus (E') measures

the material's ability to store energy during deformation, reflecting its stiffness. Loss modulus (E'') gauges the material's capacity to dissipate energy as heat during deformation, indicating its damping or energy loss characteristics. Tan delta ($\tan\delta$), the ratio of loss modulus to storage modulus, provides insight into the material's energy absorption and dissipation. The glass transition temperature (T_g) refers to the temperature at which a material transitions from a glassy to a rubbery state, affecting its mechanical properties. Lastly, the $\tan\delta$ half-height peak width (P_w) assesses the breadth of the temperature range over which the material undergoes a significant phase transition. These parameters collectively provide a comprehensive understanding of the Epoxy/Graphite composite's behavior under various conditions, facilitating practical applications and informed design considerations.

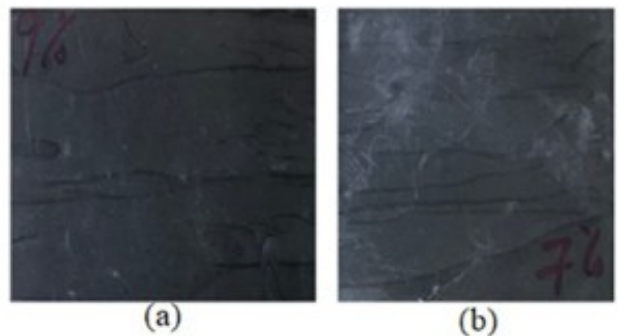


Figure 4 (a) Epoxy/Graphite wt9% (b)Epoxy/Graphite wt7%

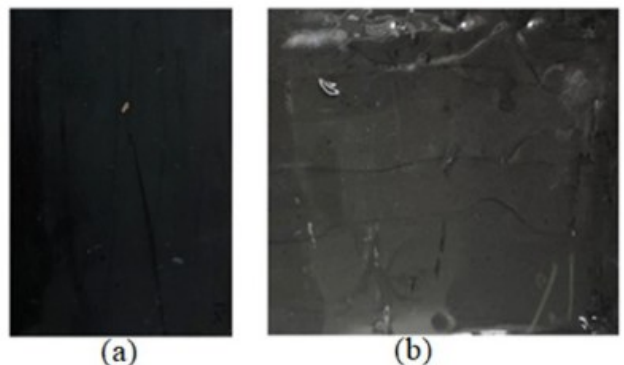


Figure 5 (a) Epoxy/Graphite wt2% mixed (b) Epoxy/graphite wt1% surface coated

In Figure 7(a), the $\tan\delta$ vs temperature plot illustrates the significant effect of the coated surface with wt.% graphite on the specimen. This effect is attributed to the structure and nature of carbon-carbon bonds, contributing to increased internal friction within the epoxy matrix. The higher internal friction results in elevated $\tan\delta$ values on surface-coated specimens, enhancing damping properties compared to mixed specimens.

Figure 7(b), the E' vs wt.% graphite plot, shows the impact of adding graphite fillers on the storage modulus of epoxy composite materials. Storage modulus, representing elastic modulus or stiffness, measures a material's ability to store elastic energy during deformation. Adding graphite fillers reduces the storage modulus for surface-coated specimens but increases it for mixed specimens. The graphite particles effectively reinforce the epoxy matrix, producing a composite with improved mechanical properties.

Figure 7(c) shows the effect on temperatures; incorporating graphite fillers into epoxy enhances the composite's thermal conductivity due to graphite's excellent thermal conduction. This improvement results in temperature-dependent behavior, influencing the tan delta.

The material's stiffness changes with temperature, and higher temperatures amplify the viscoelastic effect, as indicated in the Temperature vs wt. % of the graphite subplot in Figure 7. Considering the width of the tan- δ peak, a measure of the broadness or narrowness of the damping response, Figure 7(d) subplot of Pw vs wt. % graphite, provides valuable insights. The coated specimen exhibits high energy dissipation, unlike the mixed specimen. The influence of graphite filler on the composite's damping behavior is evident, where adding filler increases internal friction within the material, affecting the width of tan- δ .

The volume fraction concentration of the filler significantly impacts mechanical and thermal properties through interfacial interactions between graphite fillers and the material matrix. The size and distribution of graphite particles within the composites also affect material homogeneity, with the non-uniform response at wt.2.3%, showing the highest Pw among the specimens tested, as seen in Figure 7(d).

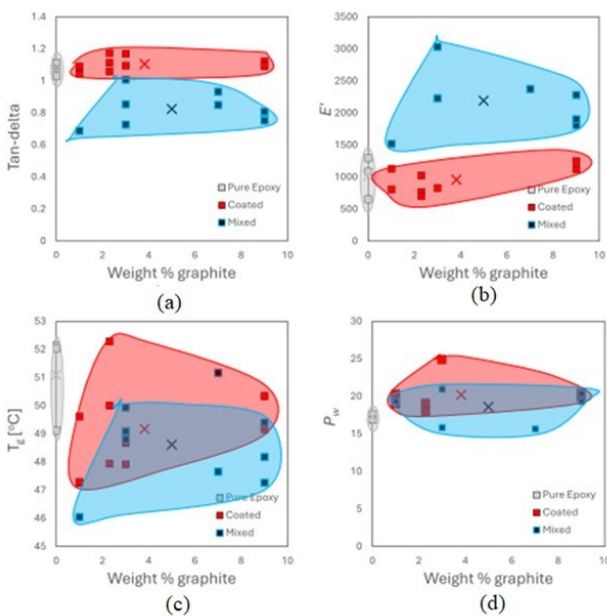


Figure 7 Effect of wt. % graphite on tan delta, temperature, loss modulus, and half-height peak width (Pw) of composite

DMA results constitute E' , E'' , $\tan-\delta$ and T_g as shown in Figure 8, comparing these values used in processing to establish heat history, residual stress, temperature and fillers effect. The specimen properties indicate transition temperatures (T_g), environment resistance, impact strength and adhesion properties. The dynamic temperature ramp provides information on the polymer's structure-property relationship.

The glass transition temperature (T_g) is the temperature at which the polymer changes from a hard, brittle material to a soft, rubbery material; this could be attributed by the carbon chains start moving in a polymer at this temperature, resulting in an

amorphous region experiencing a transition from a rigid state to a flexible state. The viscoelastic properties of a semi-crystalline polymer allow flexibility. Every polymer with an amorphous structure has a unique glass transition temperature, useful in determining whether a given material is better suited for flexible or rigid material application. The plots on figure 8 and 9 demonstrate this principle.

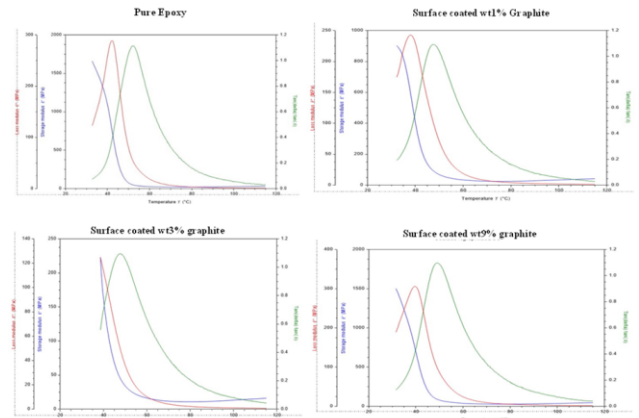


Figure 8 Surface coated wt. % graphite specimen compared with pure epoxy

Pure epoxy has values of T_g 60°C, with storage modulus of 1625MPa, Loss modulus of 275MPa, and $\tan-\delta$ of 1.15; surface coated specimen had T_g 55°C and with storage modulus ranging from 225MPa to 1500MPa with respective $\tan-\delta$ of 1.1 as seen in Figure 9. The storage modulus characterizes the elastic behavior of the material, and the loss modulus characterizes the viscous behavior of the material. At the same time, the $\tan-\delta$ is the storage and loss modulus ratio. From the results, the surface-coated specimen demonstrated more viscoelastic properties compared to pure epoxy material and a low $\tan-\delta$ value compared to epoxy material.

Mixed specimen of epoxy and graphite had T_g of 50-70°C, a storage modulus of 4750 to 70000MPa, a loss modulus from 650-25000MPa and a $\tan-\delta$ from 0.7 to 1.375. The addition of more filler to the composite increased the stiffness.

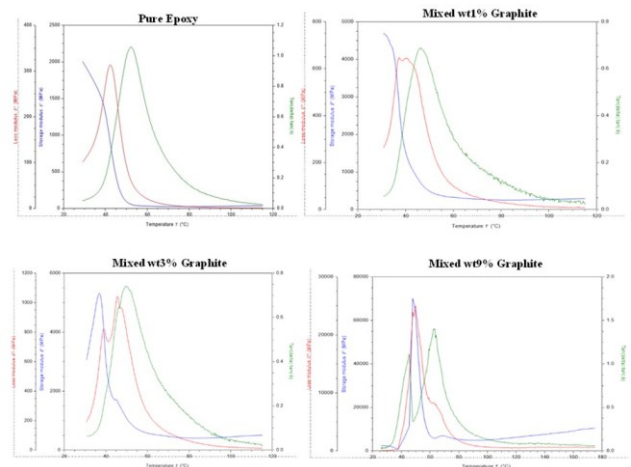


Figure 9 Mixed wt. % graphite specimen compared with pure epoxy

A low $\tan-\delta$ for a composite material indicates that it is less lossy and more elastic, meaning it has more potential to store the load rather than dissipate it.

Graphite/epoxy current measurement during tensile tests

Graphite is a highly conductive material, so when used as a coating in a composite, it enhances the overall electrical conductivity of the material, hence advantageous in applications requiring electrical conductivity. Depending on the frequency of the applied current, the composite can display various phenomena, including impedance matching or absorption of electromagnetic radiation; this is relevant in the study, especially in electromagnetic shielding or absorption of radio-frequency energy.

Graphite is corrosion-resistant, especially when exposed to harsh environmental conditions or corrosive substances. Its' coating provides protection and maintains the electrical properties of the composite for a long time. It was established that interaction between the graphite coating and the composite matrix is important as a well-bonded matrix ensures efficient electrical conductivity, poor bonding results in increased resistance and reduced effectiveness of the graphite coating.

Figure 10 shows the mean current flow in a surface-coated specimen; the higher the wt.% graphite, the increased current measured and ease of flow. This can be attributed to the interaction between electrical and mechanical behavior, which depends on the electrical conductivity of the graphite filler, composite matrix and applied current and the testing conditions. Electric current passing through a conductive material like graphite generates heat due to resistive heating, known as the joule effect. The joule influences the mechanical properties of the composite, as the temperature increases, softens the matrix material, leading to changes in the stress-strain behavior.

The extent of changes depends on the thermal properties of the filler and the matrix, leading to thermal expansion in the composite material. The expansion contributes to changes in the stress-strain curve regarding elongation and deformation. Similarly, an electric current can induce electromechanical effects in the composite.

The interaction between the electrical field and conductive phase in a composite containing graphite particle influences mechanical response. This will eventually lead to changes in stress-strain behavior in terms of conductivity-dependent effects. High electric current can lead to localized heating and thermal stress concentrations, potentially causing damage to the composite; the damage manifests in stress-strain curves such as reduced strength or increased brittleness.

In conclusion, adding graphite fillers to epoxy composites can improve their mechanical, thermal, and physical properties. However, the extent of improvement depends on the composite type and the percentage of graphite filler used summarized in Figure 10b. The coating effect on the material is demonstrated by mean stress and mean strain Figure 10. The stress-strain curve of a composite material is characterized by a critical point, beyond

which a crack will propagate and cut the sample very fast, causing an abrupt drop in the curve. Increased filler enhanced critical point of the specimen samples, especially on the surface coated ones, led to increased stress, e.g., Epoxy = 20, surface wt.%2.3 = 30, wt.%3 = 25; and wt.9% = 32, while strain values epoxy = 0.042, wt.%2.3 = 0.025; wt.%3 = 0.032; wt.%9 = 0.029; This indicates that adding graphite filler wt.% to the specimen takes more force to withstand before it breaks, consequently increasing break points.

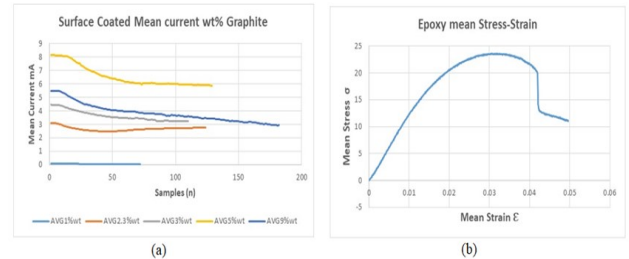


Figure 10 Surface coated current Mean wt. % graphite on stress-strain curves

Mixed wt. % graphite/epoxy specimen

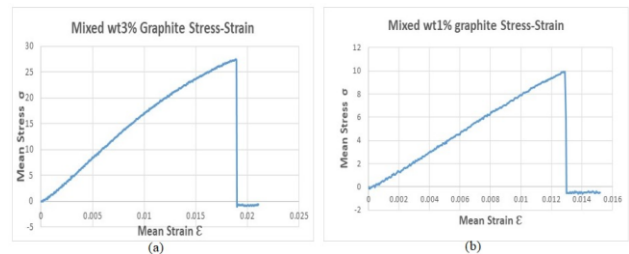


Figure 31 Mixed coated wt. % graphite Stress-strain curves

Figure 11 (a) of a mean mixed specimen of wt.% graphite, indicates the stress and strain values on mixed specimens being low, hence exhibited brittleness attributes. Consequently, at low weight percentages (1-2.3%), the graphite seems to have little influence on the tensile behavior. Intermediate weight percentage of the graphite seem optimum for mechanical performance in the epoxy composites as it slightly reduced the tensile properties and exhibited significant hardness improvement.

Sheet resistivity (Electro Static Discharge -ESD)

Sheet resistivity measures materials' electrical resistance per unit square, commonly used to characterize the conductivity of thin films or coatings. Graphite has excellent electrical conductivity; introducing graphite fillers in a composite forms a conductive network within the material.

The network facilitates the flow of electrons and reduces the overall electrical resistance to the composite, leading to lower sheet resistivity. Consequently, higher filler content results in a more conductive composite with lower sheet resistivity, although it exits the optimal range where conductivity is maximized before diminishing returns occur. Notably, the electrical conductivity of graphite, and consequently, sheet resistivity, can be influenced by temperature. Change in temperature affects the mobility of charge carriers and alters overall conductivity.

In Figure 12, the mixture specimen with the epoxy/composites' highest resistivity value is 1.75E14, hence an insulative polymer as it falls in the range of 10¹²-10¹⁶. The Insulative materials limit

flow of electrons across their surface, they exhibit high electrical resistance. While the surface coated Epoxy/graphite exhibited conductive properties composites and static dissipative characteristics with low value of resistivity. Low wt.% graphite coating increased percentage beyond wt.2%, and the composites became conductive. The concentration of graphite filler enhanced the conductivity of the composite, consequently affecting the material's dielectric behavior, influencing the material $\tan-\delta$. The Addition of graphite fillers decreases sheet resistivity due to the improved electrical conductivity.

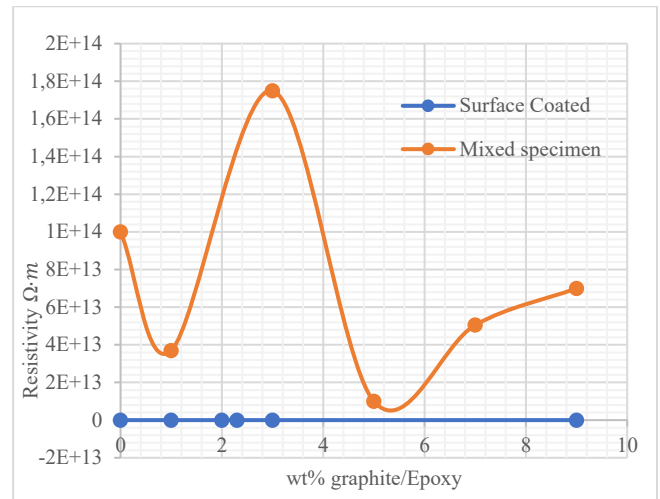


Figure 12 Sheet resistivity values of graphite/epoxy coated and Mixed surface.

Table 2. Comparison of different techniques

Technique	Type of system	Accuracy
Composite epoxy-graphite materials and their electrochemical application [34], [52]	Characterization of epoxy-graphite composites modified with benzoic acid, graphene oxide and hydrotalcite. Characterized by cyclic voltammetry, electrochemical impedance spectroscopy, and field-emission scanning electron microscopy.	Flexural tests undertaken, included other modifications of materials using benzoic acid, graphene oxide and hydrotalcite materials. The test is a different from the investigation due to modification of the composites with benzoic acid and hydrotalcite.
The Impact of Filler content on mechanical and micro-structural characterization of graphite-Epoxy composites [9]	Evaluation of Graphite/Epoxy composites (GECs) from mechanical perspectives, used different % of graphite for tensile and hardness.	The graphite has little influence on the tensile behavior. An intermediate weight % of the graphite is considered optimum for mechanical performance in the epoxy composites as it slightly reduces the tensile properties and significantly improves the hardness
Conductive materials for ESD applications: An overview [27] [53], [54].	Summary of composites materials and categories, various methods of enhancing conductivity through chemical additives.	Effect of filler loading on composite resistivity follows a nearly universal pattern regardless of which fillers are chosen. Unable to explain why resistivity follows uniform pattern for majority of resins irrespective which one is used.
Electrical and Mechanical properties of expanded graphite/HDPE nanocomposites [8], [37], [40]	Observation of morphology, diffraction of nanocomposites, tensile tests to determine tensile strength, young's modulus and elongation at break values.	Polymers cannot provide protection against ESD on sensitive electronics devices. Requires development of electrically conductive polymers or filled with conducting fillers e.g., carbon black or natural flake graphite.
The impact of filler content on mechanical and micro-structural characterization of graphite-epoxy components[9], [55].	Use of different weight % of graphite (0-7 wt.%) for tensile and hardness experiments. To ascertain the optimum mixing ratio of the graphite with the epoxy.	Amount of graphite choice impairs properties e.g., tensile strength, hardness, compressive power, conductivity, water absorption, degradation etc.
Polymer & Composites Effect of Fillers on Electrical Conductivity of Epoxy Composites [37], [56]	Comparison of Graphite (Gr), silicon carbide (SiC) and hybrid of Graphite and silicon carbide (Gr-SiC)-epoxy, electrical conductivities.	Electrical conductivity of epoxy is insignificant at lower filler fraction as particles are distributed discretely inhibiting the formation of conductive paths. Effective conductivity of composites depends on size, filler geometry and filler type.

CONCLUSIONS

This research on Epoxy/graphite composites with varying weight percentages of graphite powder as HDE substrates has illuminated their mechanical and electrical attributes. Surface-coated samples exhibited enhanced mechanical properties attributed to effective dispersion, strong interfacial interaction, and improved adhesion between epoxy and graphite. The investigation identified a critical point at wt.9% graphite content, where a substantial increase in high current flow was observed, indicating a noteworthy threshold in electrical conductivity influenced by filler content. Adding fillers to a certain weight percentage transformed the materials from insulative to conductive composites, with resistivity ranging from 10^3 - 10^5 . This versatile composite, known for its cost-effectiveness, emerges as a compelling choice, especially for applications requiring a balance between mechanical strength and electrical conductivity, in external radome layers design and fabrication. The findings suggest that Epoxy/graphite composites could be an effective and economical solution in scenarios where structural integrity and electrical performance are paramount, positioning them as promising candidates for external radome applications in various industries. A well-designed antenna radome provides environmental protection, which extends the operating lifetime of the antenna and its components. It contributes to the stable electrical performance of the system with reduced maintenance efforts and downtime, thus supporting reduced total cost of ownership. Graphite/Epoxy structures have critical weight savings, improved control of thermal distortions and increased structural stiffness. The investigation opens the future research on multi-layered radome based on SRRs metamaterials for wide and extreme applications.

ACKNOWLEDGMENT

The authors thanks Dedan Kimathi University of Technology for research's financial and material support and University of Edinburgh UK for laboratory equipment and Dr. Parvez Alam for guidance.

REFERENCES

- [1] Z. Lu, "The radome design of L-band satellite tracking vehicle antenna: innovative material selection and sealing reinforcement," 2024, Accessed: May 25, 2025. [Online]. Available: <https://lutpub.lut.fi/handle/10024/167506>
- [2] M. E. Leyva, G. M. O. Barra, A. C. F. Moreira, B. G. Soares, and D. Khastgir, "Electric, dielectric, and dynamic mechanical behavior of carbon black/styrene-butadiene-styrene composites," *J Polym Sci B Polym Phys*, vol. 41, no. 23, pp. 2983–2997, Dec. 2003, doi: 10.1002/POLB.10627.
- [3] I. Kranauskaite *et al.*, "Dielectric properties of graphite-based epoxy composites," *Wiley Online Library/I Kranauskaite, J Macutkevicius, P Kuzhir, N Volynets, A Paddubskaya, D BychanokPhysica status solidi (a)*, 2014•*Wiley Online Library*, vol. 211, no. 7, pp. 1623–1633, 2014, doi: 10.1002/PSSA.201431101.
- [4] A. Nag, R. Rao, P. P.-C. International, and undefined 2021, "High temperature ceramic radomes (HTCR)–A review," *ElsevierA Nag, RR Rao, PK PandaCeramics International*, 2021•*Elsevier*, Accessed: May 25, 2025. [Online]. Available: <https://www.sciencedirect.com/science/article/pii/S0272884221012475>
- [5] "Dielectric and mechanical properties of hypersonic radome materials and metamaterial design: A review - ScienceDirect." Accessed: May 25, 2025. [Online]. Available: <https://www.sciencedirect.com/science/article/abs/pii/S0955221921007159>
- [6] T. Kenion, N. Yang, and C. Xu, "Dielectric and mechanical properties of hypersonic radome materials and metamaterial design: A review," *J Eur Ceram Soc*, vol. 42, no. 1, pp. 1–17, Jan. 2022, doi: 10.1016/J.JEURCERAMSOC.2021.10.006.
- [7] P. Kuzhir *et al.*, "Epoxy composites filled with high surface area-carbon fillers: Optimization of electromagnetic shielding, electrical, mechanical, and thermal properties," *J Appl Phys*, vol. 114, no. 16, Oct. 2013, doi: 10.1063/1.4826529.
- [8] A. Kaushik, P. Singh, and Jyoti, "Mechanical and electrical conductivity study on epoxy/graphite composites," *journals.sagepub.comA Kaushik, P Singh, JyotiJournal of reinforced plastics and composites*, 2010•*journals.sagepub.com*, vol. 29, no. 7, pp. 1038–1044, Apr. 2010, doi: 10.1177/0731684409103055.
- [9] "The Impact of Filler Content on Mechanical and Micro-Structural Characterization of Graphite-Epoxy Composites." Accessed: May 25, 2025. [Online]. Available: <https://www.scirp.org/journal/paperinformation?paperid=117914>
- [10] V. Soumya, S. Navaneetha, ... A. R.-I. J. of, and undefined 2017, "Design considerations of radomes: a review," *academia.eduVM Soumya, S Navaneetha, AN Reddy, JJ KumarInternational Journal of Mechanical Engineering and Technology*, 2017•*academia.edu*, Accessed: May 25, 2025. [Online]. Available: https://www.academia.edu/download/52144216/IJMET_08_03_005.pdf
- [11] C. Min and D. Yu, "Simultaneously improved toughness and dielectric properties of epoxy/graphite nanosheet composites," *Polym Eng Sci*, vol. 50, no. 9, pp. 1734–1742, Sep. 2010, doi: 10.1002/PEN.21698;PAGE:STRING:ARTICLE/CHAPTER.
- [12] Y. Ren *et al.*, "Simultaneous enhancement on thermal and mechanical properties of polypropylene composites filled with graphite platelets and graphene sheets," *ElsevierY Ren, Y Zhang, H Fang, T Ding, J Li, SL BaiComposites Part A: Applied Science and Manufacturing*, 2018•*Elsevier*, Accessed: May 25, 2025. [Online]. Available: <https://www.sciencedirect.com/science/article/pii/S1359835X18301969>
- [13] B. Mayzel, L. Aram, N. Varsano, S. G. Wolf, and A. Gal, "Structural evidence for extracellular silica formation by diatoms," *Nature Communications 2021 12:1*, vol. 12,

- no. 1, pp. 1–8, Jul. 2021, doi: 10.1038/s41467-021-24944-6.
- [14] C. Nwambu, C. Robert, and P. Alam, “Dynamic mechanical thermal analysis of unaged and hygrothermally aged discontinuous Bouligand structured CFRP composites,” *Functional Composites and Structures*, vol. 4, no. 4, p. 045001, Oct. 2022, doi: 10.1088/2631-6331/AC99D2.
- [15] K. P. Menard and N. R. Menard, “DMA Applications to Real Problems: Guidelines,” *Dynamic Mechanical Analysis*, pp. 237–252, May 2020, doi: 10.1201/9780429190308-10/DMA-APPLICATIONS-REAL-PROBLEMS-GUIDELINES-KEVIN-MENARD-NOAH-MENARD.
- [16] A. Sihvola, “Metamaterials in electromagnetics,” *Metamaterials*, vol. 1, no. 1, pp. 2–11, Mar. 2007, doi: 10.1016/j.metmat.2007.02.003.
- [17] M. Saeedi Heydari, J. Ghezavati, M. Abbasgholipour, and B. Mohammadi Alasti, “Various types of ceramics used in radome: A review,” *Scientia Iranica*, vol. 24, no. 3, pp. 1136–1147, Jun. 2017, doi: 10.24200/SCI.2017.4095.
- [18] N. Khatavkar and K. Balasubramanian, “Composite materials for supersonic aircraft radomes with ameliorated radio frequency transmission-a review,” 2016, *Royal Society of Chemistry*. doi: 10.1039/c5ra18712e.
- [19] J. Varghese, N. Joseph, H. Jantunen, S. K. Behera, H. T. Kim, and M. T. Sebastian, “Microwave Materials for Defense and Aerospace Applications,” in *Handbook of Advanced Ceramics and Composites: Defense, Security, Aerospace and Energy Applications*, Springer International Publishing, 2020, pp. 165–213. doi: 10.1007/978-3-030-16347-1_9.
- [20] H. Yang *et al.*, “Preparation and properties of porous silicon nitride ceramics with polymethyl methacrylate as pore-forming agent,” *Ceram Int*, vol. 46, no. 10, pp. 17122–17129, Jul. 2020, doi: 10.1016/J.CERAMINT.2020.03.204.
- [21] Y. Wu *et al.*, “Influence of the content of polymethyl methacrylate on the properties of porous Si₃N₄ ceramics fabricated by digital light processing,” *Elsevier YR Wu, C Tian, JM Wu, HL Huang, CL Liu, X Lin, LJ Cheng, YS Shi Ceramics International, 2023*•Elsevier, Accessed: May 25, 2025. [Online]. Available: <https://www.sciencedirect.com/science/article/pii/S0272884223019958>
- [22] K. Bilisik, M. A.-J. of M. Science, and undefined 2022, “Polymer nanocomposites based on graphite nanoplatelets (GNPs): a review on thermal-electrical conductivity, mechanical and barrier properties,” *Springer K Bilisik, M Akter Journal of Materials Science, 2022*•Springer, vol. 57, no. 15, pp. 7425–7480, Apr. 2022, doi: 10.1007/S10853-022-07092-0.
- [23] W. K. Goertzen and M. R. Kessler, “Dynamic mechanical analysis of carbon/epoxy composites for structural pipeline repair,” *Composites B*, vol. 38, no. 1, pp. 1–9, Jan. 2007, doi: 10.1016/j.compositesb.2006.06.002.
- [24] A. Franck, T. G.-T. Instruments, N. Castle, undefined DE, undefined USA, and undefined 1993, “Viscoelasticity and dynamic mechanical testing,” *tainstruments.com A Franck, TI Germany TA Instruments, New Castle, DE, USA AN004, 1993*•tainstruments.com, Accessed: May 25, 2025. [Online]. Available: <https://www.tainstruments.com/pdf/literature/AAN004.pdf>
- [25] C. K. Schoff, “Dynamic mechanical analysis,” *Coatings Tech*, vol. 5, no. 10, p. 44, May 2008, doi: 10.1201/9780429190308/DYNAMIC-MECHANICAL-ANALYSIS-KEVIN-MENARD-NOAH-MENARD/RIGHTS-AND-PERMISSIONS.
- [26] K. Roy, Md. N. Alam, S. K. Mandal, and S. C. Debnath, “Silica-coated nano calcium carbonate reinforced polychloroprene rubber nanocomposites: influence of silica coating on cure, mechanical and thermal properties,” *J Nanostructure Chem*, vol. 6, pp. 15–24, Nov. 2015, doi: 10.1007/s40097-015-0174-x.
- [27] R. R.-I. transactions on device and materials and undefined 2002, “Conductive materials for ESD applications: an overview,” *ieeexplore.ieee.org RB Rosner IEEE transactions on device and materials reliability, 2002*•ieeexplore.ieee.org, Accessed: May 25, 2025. [Online]. Available: <https://ieeexplore.ieee.org/abstract/document/946455/>
- [28] L. Du and S. C. Jana, “Hygrothermal effects on properties of highly conductive epoxy/graphite composites for applications as bipolar plates,” *J Power Sources*, vol. 182, no. 1, pp. 223–229, Jul. 2008, doi: 10.1016/J.JPOWSOUR.2008.03.071.
- [29] M. S. Heydari, J. Ghezavati, M. Abbasgholipour, and B. M. Alasti, “Various types of ceramics used in radome: A review,” *Scientia Iranica, Transactions B: Mechanical Engineering*, vol. 24, pp. 1136–1147, 2017.
- [30] T. O. Abreu *et al.*, “A novel ceramic matrix composite based on YNbO₄-TiO₂ for microwave applications,” *Ceram Int*, vol. 47, no. 11, pp. 15424–15432, Jun. 2021, doi: 10.1016/j.ceramint.2021.02.108.
- [31] R. I. Corona *et al.*, “Nested helicoids in Bouligand microstructures,” *Nat. Commun.*, vol. 11, no. 1, p. 224, Dec. 2020, doi: 10.1038/s41467-020-15951-0.
- [32] Y. Kim, Y. Qian, M. Kim, J. Ju, S. H. Baek, and S. E. Shim, “A one-step process employing various amphiphiles for an electrically insulating silica coating on graphite,” *RSC Adv*, vol. 7, no. 39, pp. 24242–24254, May 2017, doi: 10.1039/C7RA03049E.
- [33] C. N. Nwambu, C. Robert, and P. Alam, “Viscoelastic properties of bioinspired asymmetric helicoidal CFRP composites,” *MRS Adv.*, vol. 7, no. 31, pp. 805–810, Nov. 2022, doi: 10.1557/s43580-022-00332-0.
- [34] S. Bellucci *et al.*, “Microstructure, elastic and electromagnetic properties of epoxy-graphite composites,” *AIP Adv*, vol. 5, no. 6, Jun. 2015, doi: 10.1063/1.4922872/639.
- [35] B. B. Johnsen, A. J. Kinloch, R. D. Mohammed, A. C. Taylor, and S. Sprenger, “Toughening mechanisms of nanoparticle-modified epoxy polymers,” *Polymer (Guildf)*, vol. 48, no. 2, pp. 530–541, Jan. 2007, doi: 10.1016/J.POLYMER.2006.11.038.
- [36] M. D. Zahidul Islam, Y. Fu, H. Deb, M. D. Khalid Hasan, Y. Dong, and S. Shi, “Polymer-based low

- dielectric constant and loss materials for high-speed communication network: Dielectric constants and challenges,” *Eur Polym J*, vol. 200, Nov. 2023, doi: 10.1016/j.eurpolymj.2023.112543.
- [37] R. Sengupta, M. Bhattacharya, S. Bandyopadhyay, and A. K. Bhowmick, “A review on the mechanical and electrical properties of graphite and modified graphite reinforced polymer composites,” *Progress in Polymer Science (Oxford)*, vol. 36, no. 5, pp. 638–670, May 2011, doi: 10.1016/J.PROGPOLYMSCI.2010.11.003.
- [38] A. de A. P. Gabino, T. Indrusiak, and B. G. Soares, “Evaluation of Thermoplastic Vulcanizates in Radomes,” *Journal of Aerospace Technology and Management*, vol. 11, 2019, doi: 10.5028/jatm.etmq.11.
- [39] N. Khatavkar and B. K., “Composite materials for supersonic aircraft radomes with ameliorated radio frequency transmission-a review,” *RSC Adv*, vol. 6, pp. 6709–6718, 2016, doi: 10.1039/c5ra18712e.
- [40] K. Sever, I. Tavman, Y. Seki, ... A. T.-C. P. B., and undefined 2013, “Electrical and mechanical properties of expanded graphite/high density polyethylene nanocomposites,” *ElsevierK Sever, IH Tavman, Y Seki, A Turgut, M Omasstova, I OzdemirComposites Part B: Engineering, 2013•Elsevier*, Accessed: May 25, 2025. [Online]. Available: <https://www.sciencedirect.com/science/article/pii/S1359836813002266>
- [41] K. Karvanis, S. Rusnáková, M. Žaludek, and A. Čapka, “Preparation and Dynamic Mechanical Analysis of Glass or carbon Fiber/Polymer Composites,” *IOP Conf Ser Mater Sci Eng*, vol. 362, no. 1, p. 012005, May 2018, doi: 10.1088/1757-899X/362/1/012005.
- [42] N. Pytlik and E. Brunner, “Diatoms as potential ‘green’ nanocomposite and nanoparticle synthesizers: challenges, prospects, and future materials applications,” *MRS Commun*, vol. 8, no. 2, pp. 322–331, Jun. 2018, doi: 10.1557/MRC.2018.34.
- [43] A. Kaushik, P. Singh, and Jyoti, “Mechanical and Electrical Conductivity Study on Epoxy/Graphite Composites,” *Journal of Reinforced Plastics and Composites*, vol. 29, pp. 1038–1044, Nov. 2009, doi: 10.1177/0731684409103055.
- [44] N. Pytlik and E. Brunner, “Diatoms as potential ‘green’ nanocomposite and nanoparticle synthesizers: challenges, prospects, and future materials applications,” *MRS Commun*, vol. 8, pp. 322–331, Nov. 2018, doi: 10.1557/mrc.2018.34.
- [45] J. Zhang and S. Qi, “Mechanical, thermal, and dielectric properties of aluminum nitride/glass fiber/epoxy resin composites,” *Polym Compos*, vol. 35, no. 2, pp. 381–385, Feb. 2014, doi: 10.1002/PC.22671.
- [46] C. Esposito Corcione and A. Maffezzoli, “Transport properties of graphite/epoxy composites: Thermal, permeability and dielectric characterization,” *Polym Test*, vol. 32, no. 5, pp. 880–888, 2013, doi: 10.1016/J.POLYMERTESTING.2013.03.023.
- [47] F. Zhang, J. Xu, G. Xu, L. Z.-C. Structures, and undefined 2017, “The buckling behavior of radome with different braided angles based on CFRP,” *ElsevierF Zhang, J Xu, G Xu, L ZuComposite Structures, 2017•Elsevier*, Accessed: May 25, 2025. [Online]. Available: <https://www.sciencedirect.com/science/article/pii/S0263822317314630>
- [48] K. Roy, M. N. Alam, S. K. Mandal, and S. C. Debnath, “Silica-coated nano calcium carbonate reinforced polychloroprene rubber nanocomposites: influence of silica coating on cure, mechanical and thermal properties,” *SpringerK Roy, MN Alam, SK Mandal, SC DebnathJournal of Nanostructure in Chemistry, 2016•Springer*, vol. 6, no. 1, pp. 15–24, Mar. 2016, doi: 10.1007/S40097-015-0174-X.
- [49] M. Pacios, M. Del Valle, ... J. B.-J. of E., and undefined 2008, “Electrochemical behavior of rigid carbon nanotube composite electrodes,” *Elsevier*, Accessed: May 25, 2025. [Online]. Available: <https://www.sciencedirect.com/science/article/pii/S002072808001423>
- [50] K. P. Menard and N. R. Menard, “Dynamic Testing and Instrumentation,” *Dynamic Mechanical Analysis*, pp. 85–110, May 2020, doi: 10.1201/9780429190308-5/DYNAMIC-TESTING-INSTRUMENTATION-KEVIN-MENARD-NOAH-MENARD.
- [51] . M. K. G. and . K. R., “Multi layers glass fibres reinforced epoxy composite: dynamic mechanical analysis,” *Advanced Materials Proceedings*, vol. 2, no. 8, pp. 518–520, Dec. 2017, doi: 10.5185/amp.2017/810.
- [52] O. S. Yakovenko *et al.*, “Epoxy composites filled with graphite nanoplatelets modified by FeNi nanoparticles: Structure and microwave properties,” *Materials Science and Engineering: B*, vol. 283, 2022, doi: 10.1016/j.mseb.2022.115776.
- [53] S. Jiang *et al.*, “Comparison of compressive strength and electrical resistivity of cementitious composites with different nano- and micro-fillers,” *Archives of Civil and Mechanical Engineering*, vol. 18, no. 1, 2018, doi: 10.1016/j.acme.2017.05.010.
- [54] H. Liu, A. Deshmukh, N. Salowitz, J. Zhao, and K. Sobolev, “Resistivity Signature of Graphene-Based Fiber-Reinforced Composite Subjected to Mechanical Loading,” *Front Mater*, vol. 9, 2022, doi: 10.3389/fmats.2022.818176.
- [55] A. Shalwan, F. M. Alajmi, N. Alajmi, A. Shalwan, F. M. Alajmi, and N. Alajmi, “The Impact of Filler Content on Mechanical and Micro-Structural Characterization of Graphite-Epoxy Composites,” *Journal of Materials Science and Chemical Engineering*, vol. 10, no. 6, pp. 19–29, Jun. 2022, doi: 10.4236/MSCE.2022.106003.
- [56] B. Krause, P. Rzecczkowski, and P. Pötschke, “Thermal conductivity and electrical resistivity of melt-mixed polypropylene composites containing mixtures of carbon-based fillers,” *Polymers (Basel)*, vol. 11, no. 6, 2019, doi: 10.3390/POLYM11061073.

NOMENCLATURE

- ρ specific resistivity of the conductor,
 σ specific conductivity of the conductor,
 f frequency,
 ω angular frequency and

μ magnetic permeability, this formular is used to compute transmitted power through a conductor.

D maximum linear dimension of the radar antenna

λ wavelength

Γ reflection coefficient

τ Transmission coefficient

E_r Reflected electric field strength

E_i Incident electric field strength

E_t Transmitted electric field strength

ϵ_1 medium 1 dielectric property

ϵ_2 medium 2 dielectric property.

t_{optimum} Optimum thickness of radome wall or target thickness to make the radome transparent.

n: 1, 2, 3...

λ_m wavelength of the material

C speed of light

ϵ_r relative permittivity